


Glycine Receptor Autoantibodies Impair Receptor Function and Induce Motor Dysfunction

Vera Rauschenberger,^{1†} Niels von Wardenburg,^{1†} Natascha Schaefer,¹ Kazutoyo Ogino,² Hiromi Hirata,² Christina Lillesaar,³ Christoph J. Kluck,⁴ Hans-Michael Meinck,⁵ Marc Borrmann,⁶ Andreas Weishaupt,⁷ Kathrin Doppler,⁷ Jonathan Wickel,⁸ Christian Geis,⁸ Claudia Sommer,⁷ and Carmen Villmann ¹

Objective: Impairment of glycinergic neurotransmission leads to complex movement and behavioral disorders. Patients harboring glycine receptor autoantibodies suffer from stiff-person syndrome or its severe variant progressive encephalomyelitis with rigidity and myoclonus. Enhanced receptor internalization was proposed as the common molecular mechanism upon autoantibody binding. Although functional impairment of glycine receptors following autoantibody binding has recently been investigated, it is still incompletely understood.

Methods: A cell-based assay was used for positive sample evaluation. Glycine receptor function was assessed by electrophysiological recordings and radioligand binding assays. The *in vivo* passive transfer of patient autoantibodies was done using the zebrafish animal model.

Results: Glycine receptor function as assessed by glycine dose–response curves showed significantly decreased glycine potency in the presence of patient sera. Upon binding of autoantibodies from 2 patients, a decreased fraction of desensitized receptors was observed, whereas closing of the ion channel remained fast. The glycine receptor N-terminal residues ²⁹A to ⁶²G were mapped as a common epitope of glycine receptor autoantibodies. An *in vivo* transfer into the zebrafish animal model generated a phenotype with disturbed escape behavior accompanied by a reduced number of glycine receptor clusters in the spinal cord of affected animals.

Interpretation: Autoantibodies against the extracellular domain mediate alterations of glycine receptor physiology. Moreover, our *in vivo* data demonstrate that the autoantibodies are a direct cause of the disease, because the transfer of human glycine receptor autoantibodies to zebrafish larvae generated impaired escape behavior in the animal model compatible with abnormal startle response in stiff-person syndrome or progressive encephalitis with rigidity and myoclonus patients.

ANN NEUROL 2020;88:544–561

View this article online at [wileyonlinelibrary.com](https://onlinelibrary.wiley.com/doi/10.1002/ana.25832). DOI: 10.1002/ana.25832

Received Mar 17, 2019, and in revised form Jun 23, 2020. Accepted for publication Jun 23, 2020.

Address correspondence to Dr Villmann, Institute for Clinical Neurobiology, Julius Maximilian University of Würzburg, Versbacherstrasse 5, D-97078 Würzburg, Germany. E-mail: villmann_c@ukw.de

[†]V.R. and N.v.W. contributed equally to this work.

From the ¹Institute for Clinical Neurobiology, University Hospital, Julius Maximilian University of Würzburg, Würzburg, Germany; ²Department of Chemistry and Biological Science, College of Science and Engineering, Aoyama Gakuin University, Tokyo, Japan; ³Department of Child and Adolescent Psychiatry, Center of Mental Health, University Hospital of Würzburg, Würzburg, Germany; ⁴Institute of Biochemistry, Emil Fischer Center, Friedrich Alexander University Erlangen–Nürnberg, Erlangen, Germany; ⁵Department of Neurology, University Hospital Heidelberg, Heidelberg, Germany; ⁶Witten, Helios University Hospital Wuppertal, Department of Nephrology and Rheumatology, Witten/Herdecke University, Germany; ⁷Department of Neurology, University Hospital Würzburg, Würzburg, Germany; and ⁸Section of Translational Neuroimmunology, Department of Neurology, Jena University Hospital, Jena, Germany

Additional supporting information can be found in the online version of this article.

Patients with glycine receptor (GlyR) autoantibodies suffer from complex neurological disorders comprising muscle stiffness, spasms, exaggerated startle, and different forms of phobias bracketed together as stiff-person spectrum disorders.^{1–3} Severe cases of stiff-person syndrome (SPS) have been described associated with progressive encephalitis with rigidity and myoclonus (PERM).^{4–6} Chronic manifestations of autoimmune encephalitis in general develop due to autoantibodies that target synaptic receptors, neuronal surface proteins. Autoantibodies impair surface expression of targeted receptors, block receptor function, interfere with synaptic protein–protein interactions, or alter synapse formation.⁷ Symptoms of patients carrying autoantibodies against GlyRs resemble symptoms of patients harboring a GlyR mutation associated with the neurological disorder hyperekplexia (Online Mendelian Inheritance in Man database 149400).⁸

SPS is characterized by typical symptoms including limb and trunk rigidity, muscle spasms, brainstem signs, and hyperekplexia.^{5,9–12} SPS variants include focal or segmental SPS, jerking SPS, and PERM. Most patients with SPS carry autoantibodies directed against glutamic acid decarboxylase 65 (GAD65), the rate-limiting enzyme for the production of the neurotransmitter γ -aminobutyric acid.⁶ GlyR autoantibodies and amphiphysin autoantibodies are less frequent, but coexistence of GAD and GlyR autoantibodies has been described for 15% of SPS patients.^{6,13} In some patients, SPS is paraneoplastic.

The onset of SPS/PERM associated with GlyR autoantibodies and the disease pattern are highly variable. The motor system is predominantly affected, and symptoms include muscle stiffness, rigidity, spasms or myoclonus, eye movement, and bulbar disturbance, but also excessive startle, pain, autonomic disturbances, seizures, and cognitive impairment.⁴

At the molecular level, enhanced internalization of GlyRs was suggested as a possible underlying pathology mechanism. GlyR autoantibodies bind to primary neurons and to spinal cord tissue.⁴ No preference for any of the GlyR α subunits was detectable. Very recently, functional impairment of spinal cord glycine receptors was demonstrated following autoantibody binding.¹⁴

The targeted GlyRs enable fast synaptic inhibition in adult spinal cord and brainstem. The major subunit compositions in the adult organism are $\alpha 1\beta$ and $\alpha 3\beta$ receptor heteromers.¹⁵ These subunits form pentameric glycine-gated chloride channels,^{16,17} which are anchored at synapses by the scaffold protein gephyrin.¹⁸ Each GlyR subunit consists of a large extracellular domain (ECD), 4 transmembrane domains (TMs) connected by intra- or extracellular loop structures (TM1-2 loop, TM2-3 loop, TM3-4 loop), and a short extracellular C-terminus.^{19–21}

Here, we make use of blood samples (serum) from 6 patients with SPS supposed to harbor GlyR autoantibodies. Following positive evaluation of GlyR autoantibodies in all samples, we investigate whether the GlyR autoantibodies affect GlyR functionality and thus contribute to disease pathology. Furthermore, we elucidate the pathological role of GlyR autoantibodies after transfer into an in vivo animal model.

Materials and Methods

Patients

We used 6 patient sera positive for GlyR $\alpha 1$ autoantibodies (1 female, 5 males; referred to as pat1, pat2, pat3, pat4, pat5, and pat6 in the present study) for functional investigation. Three patients were diagnosed with SPS and 3 patients with PERM. Clinical symptoms can be summarized as muscular rigidity and spasms involving the paraspinal, abdominal, and lower limb muscles (Table 1). Some of the patients responded well to plasma exchange, however, with relapses.²²

Ethical Statement

Experiments using patient material have been approved by the ethics committee of the Medical Faculty of the University of Würzburg, Germany for the project “Autoantibodies and Glycinergic Dysfunction—Pathophysiology of Associated Motor Disorders.”

Purification of the Antibody-Containing IgG Fractions

Plasma filtrate was obtained during therapeutic plasmapheresis from patients with SPS or PERM. After removing fibrinogen, plasma samples were applied to a gel filtration column stocked with Sephacryl S-300 HR (GE Healthcare, Munich, Germany) equilibrated with buffer as described below.^{12,23} The total IgG concentration of the various fractions was measured by nephelometry. Fractions containing IgG were further purified by affinity chromatography using GammaBind G Sepharose (GE Healthcare). The pooled IgG fractions were applied to a column stocked with GammaBind G Sepharose and equilibrated with 0.01M sodium phosphate, 0.15M NaCl, 0.01M ethylenediaminetetraacetic acid, pH 7.0. Adsorbed material was eluted with acetic acid adjusted to pH 3.0 with ammonium hydroxide. The eluted fractions were neutralized with 2M Tris.

Fractions containing purified IgG were concentrated by passing the eluate through an Amicon Ultra 100 K filter (Merck, Darmstadt, Germany) under nitrogen (N₂) pressure to a volume of 50ml and dialysed 4 times against 10l water, to elute peptides and other low-molecular-weight components. The IgG samples were then freeze-dried and stored at -80°C until use.

Plasmids

The current study used the following cDNAs for analysis: pEGFP-N1 (Clontech/Takara, Mountain View, CA), GlyR $\alpha 1^{\text{hs}}$ -pRK5 (hs = *Homo sapiens*; accession number: AAI14948; P.Seeburg,

TABLE 1. Clinical Data of Analyzed Patients

Characteristic	Patient 1	Patient 2	Patient 3	Patient 4	Patient 5	Patient 6
Sex/age	F/54	M/52	M/63	M/37	M/34	M/76
Diagnosis	SPS	SPS	PERM	SPS	PERM	PERM
Symptoms	Lower limb stiffness, spasticity and paresis, falls, startle	Myoclonic jerks of trunk and legs, exaggerated head retraction, acoustic startle reflex violent	Myoclonus, tetraparesis, stiffness, dysphagia, autonomic failure	Lockjaw, limb stiffness, falls	Subacute onset of limb, oculomotor, and bulbar weakness with myoclonus, touch-sensitive spasms	Myoclonic jerks, stiffness, leg pain, paraparesis, autonomic failure, somnolence
Electrophysiology	Orbicularis oculi blink reflex: myoclonic synchronization	SEP, BAEP, MEP, masseter reflex inhibition normal, EMG polymyography: tactile reflex myoclonus	Not done	Lack of silent period in masseter inhibitory reflex	Not done	SEP with central lesion, AEP without potentials
CSF abnormalities	None	45 lymphocytes per μ l	30 lymphocytes per μ l	Mild increase in protein and albumin	None	Mild increase in lactate
GlyR-AB	Positive	Positive	Positive	Positive	Positive	Positive
GAD-AB	1:10,000	Negative	Negative	Negative	Negative	57,454IU/ml
Other ABs	Islet cell	Thyroglobulin, gephyrin	Negative	Negative	Negative	Islet cells (1:100)
Cancer history	None	None	Pleomorphic adenoma of parotid gland	None	Thymoma	None
Immunotherapy	PEx, St	PEx, St	St, IVIG, PEx, RTX, AZA	PEx	PEx	St, IVIG, MTX, CYC, PEx, BORT
Supportive therapy	Clonazepam	Clonazepam	Diazepam	Clonazepam		Benzodiazepines, baclofen, sedation with PR, MID, SUF, DEXM, ISO, dronabinol
mRS maximum/final	4/3	4/1	4/2	3/2	6/6	6/6
Course of disease	Chronic	Relapsing	Monophasic	Relapsing	Progressive, fatal	Progressive, fatal

Modified ranking scale²⁵: 0, no symptoms; 1, no significant disability; 2, slight disability; 3, moderate disability; 4, moderately severe disability; 5, severe disability; 6, dead.

AB = antibody; AEP = auditory evoked potential; AZA = azathioprine; BORT = bortezoimib; BAEP = brain stem auditory evoked potential; CSF = cerebrospinal fluid; CYC = cyclophosphamide; DEXM = dexmedetomidine; EMG = electromyographic; F = female; GAD = glutamic acid decarboxylase; ISO = isoflurane; IVIG = intravenous immunoglobulins; M = male; MEP = motor evoked potential; MID = midazolam; mRS = modified Rankin Scale; MTX = methotrexate; PERM = progressive encephalitis with rigidity and myoclonus; PEx = plasma exchange; PR = propofol; RTX = rituximab; SEP = sensory evoked potential; SPS = stiff-person syndrome; St = steroids; SUF = sufentanil.

Heidelberg, Germany), gephyrin–green fluorescent protein (GFP) tagged geph-eGFPC2,²⁴ and GlyR variants of the zebrafish GlyR α 1^{dr}-pCS2 (dr = *Danio rerio*, accession number: NP_571477), GlyR α 2^{dr}-pCS2 (accession number: NP_001161371), GlyR α 3^{dr}-pCS2 (accession number: NP_694497), GlyR α 4a^{dr}-pCS2 (accession number: NP_571857), GlyR α 4b^{dr}-pCS2 (accession number: NP_001189440), GlyR β a^{dr}-pCS2 (accession number: NP_571856), and GlyR β b^{dr}-pCS2 (accession number: NP_001003587; all zebrafish constructs were made from the zebrafish AB strain embryo, a generous gift from H. Hirata, Tokyo, Japan).

Glycine Receptor α 1 Variants

For the generation of a chimeric (ch) GlyR α 1 construct (GlyR α 1^{ch}) of GlyR α 1^{hs} and GlyR α 1^{dr}, a silent mutation (177A→C; amino acid P59 CCA→CCC) in GlyR α 1^{dr} was introduced by overlap extension polymerase chain reaction (PCR) mutagenesis generating a PpuM I restriction site (already present in the human GlyR α 1) to allow an easy exchange of the N-terminal domain. GlyR α 1^{ch} was sequenced across the PCR-generated sequence (LGC Genomics, Berlin, Germany).

Cell Lines

The human cell line HEK293 (human embryonic kidney, CRL-1573, ATCC, Wesel, Germany) was used for all in vitro experiments.

Transfection of Cells

HEK293 cells grown in minimum essential media (Life Technologies, Darmstadt, Germany) supplemented with 10% fetal calf serum, L-glutamine (200mM), 100U/ml penicillin, and 100 μ g/ml streptomycin were transfected using a calcium phosphate precipitation method.²⁶ In brief, at a confluency of 75%, HEK293 cells were transiently transfected with 1 μ g cDNA per 3cm dish with typically 200,000 cells seeded. Cotransfections with GFP were always performed in a 1:1 ratio using 1 μ g of each plasmid. Cells were incubated with the transfection mixture for 6 hours, washed, and supplied with fresh medium. Experiments were done 48 hours after transfection, if not stated otherwise. For ligand binding assays in a 96-well plate format, GlyR α 1^{hs} was transfected using Lipofectamine 2000 according to the manufacturer's instructions (Thermo Fisher Scientific, Waltham, MA).

Western Blot and Immunostaining

In brief, 200ng/ μ l purified GlyR α 1¹⁻²¹⁹ ECD²⁷ was loaded on 11% polyacrylamide gels and transferred to nitrocellulose membranes for 1 hour at 200mA. The membrane was blocked for 1 hour in 5% milk powder solved in Tris-buffered saline/1% Tween 020. Primary antibodies were: pat1 serum 1:50 diluted in blocking solution, pat1 purified IgG 0.2mg/ml, disease control patient (suffering from multiple sclerosis) purified IgG 0.2mg/ml, pan-GlyR antibody mAb4a 1:500. Horseradish peroxidase-linked secondary antibody goat antihuman or goat antimouse (1:15,000; 109–035-088, 115–035-146, Dianova, Hamburg, Germany) were used.

Experimental Design

Experiments involving patient sera and control sera from healthy individuals were done blinded. Data obtained for receptor binding, functional data using electrophysiological recordings, and ligand binding tests were always performed by 2 persons independently. Data obtained from zebrafish behavior studies were analyzed by 5 persons blinded. The mean of all data is shown.

Immunostaining and Antibody Competition

Living HEK293 cells were incubated for 1 hour at 4°C with either GlyR α 1-specific/pan-GlyR antibodies mAb2b/mAb4a (cat. no. 146 111/146 011, mouse IgG₁, 1:500/1:250; Synaptic Systems, Göttingen, Germany), patient sera derived from therapeutic plasma exchange material (1:50), purified IgG of pat1 serum (pat1_{IgG}; 1:50), or patient cerebrospinal fluid (CSF; 1:10) diluted in cell culture medium. After fixation using 4% paraformaldehyde/4% sucrose in phosphate-buffered saline (PBS; pH 7.4) for 20 minutes at 4°C and blocking with 5% goat serum (P30-1001, Pan Biotech, Aidenbach, Germany) in PBS for 30 minutes at 20°C, cells were incubated with secondary antibodies goat antimouse Cy3/Cy5 or goat antihuman Cy3 (1:500; Dianova). Incubation with mAb4a required an additional permeabilization step with PBS plus 0.2% (vol/vol) Triton-X 100. For competition experiments, transfected cells were incubated at 4°C either for 2 hours with pat1 serum and mAb2b simultaneously or successively for 1 hour (pat1 serum 1:50 and mAb2b 1:50, 1:100, 1:500, 1:1,000, or 1:2,000) in cell culture medium.

Radioligand-Binding Assay

Crude cell membranes were prepared from transfected cells as described previously.²⁸ Membranes preincubated with patient or control serum were incubated for 30 minutes with cold strychnine (1, 3, 10, 30, 100, 300, 1,000nM) or buffer B (25mM potassium phosphate buffer, 200mM KCl). Another 30-minute incubation followed with 3nM [³H] strychnine (30Ci/mmol; DuPont Nen, Waltham, MA). This time window is the replacement period between cold strychnine in various concentrations and labeled strychnine. Samples were loaded on GF/C (glass microfibre filters, GE Healthcare, Munich, Germany) preincubated with buffer B plus 0.5% bovine serum albumin and washed twice before drying. Dried filters were incubated with 5ml of scintillation solution and counted.

Plates (96 wells) were coated for 1 hour with 0.2% gelatin solution, treated with 0.5% glutaraldehyde solution for 15 minutes, and washed with PBS. Living HEK293 cells were incubated with pat1 serum or healthy control (1:50), mAb2b (1:500), or Hank balanced salt solution (in mM: 137 cholineCl, 5.4 KCl, 0.34 K₂HPO₄, 0.44 KH₂PO₄, 0.41 MgSO₄, 0.49 MgCl₂, 1.07 CaCl₂, 5.6 D-glucose, 10 hydroxyethylpiperazine ethane sulfonic acid, pH 7.4) as negative control for 1 hour on ice. Samples were supplemented for 30 minutes with 30mM glycine and replaced by increasing concentrations of [³H] strychnine (0, 1, 3, 10, 30, 100, 300nM; diluted in buffer B). Samples were washed and lysed with cold water. The amount of bound radioligand of the cell lysates was determined by using a

scintillation counter (Packard Tri-Carb Liquid Scintillation Counter, PerkinElmer, Rodgau, Germany). Binding data were analyzed using a nonlinear algorithm provided by the program Origin 9.0 (OriginLab Corporation, Northampton, MA).

Electrophysiological Recordings

Electrophysiological recordings were performed in whole-cell mode using the patch-clamp technique as described.²⁹ Prior to patch-clamp experiments, transfected cells were preincubated in mAb2b (1:500), patient sera (1:50), or healthy control sera (1:10) for 1 hour at 22°C. Glycine was applied using a concentration series of 1, 3, 10, 30, 100, 300, 1,000 μM diluted in external buffer using the Octaflow II system (ALA Scientific Instruments, Farmingdale, NY). Desensitization analysis was done as described.²⁹ The decaying current phase was analyzed using a single exponential function plus a constant, as shown in Equation 1:

$$I_{obs} = I_1 * e^{(-t/\tau_1)} + I_{const} \quad (1)$$

where the observed total current amplitude is I_{obs} , the fraction of current desensitizing is I_1 with time constant τ_1 , and I_{const} is the amplitude of the nondesensitizing current fraction. Desensitization behavior was described by a single exponential decay plus a constant term. The estimated functional constants of the expressed GlyRs were compared using a t test. A probability of error of $p < 0.05$ was considered significant.

In Vivo Experiments with Zebrafish

Fertilized eggs of wild-type zebrafish (*D. rerio*) matings were raised at 28.5°C on a 14-hour light/10-hour dark cycle. All experimental procedures and husbandry were in accordance with the animal care and use committee of Aoyama Gakuin University, Japan, and the animal welfare regulations of the district government of Lower Franconia, Germany.

Zebrafish larvae (56 hours postfertilization [hpf]) were anesthetized with tricaine and placed into a drop of 3% methylcellulose in a dorsal-up posture. A small hole was made on the head by removing skin above the 4th ventricle using a glass needle. After washing with artificial cerebrospinal fluid (ACSF) buffer (in mM: 100 NaCl, 2.46 KCl, 1 MgCl₂, 0.44 NaH₂PO₄, 1.13 CaCl₂, 5 NaHCO₃, 10 glucose, pH 7.2), the treated larvae were immersed in ACSF containing either 1% healthy control serum, 1% patient serum, 1% serum containing GAD antibodies, or 1 mg/ml purified IgG. After 16 hours, escape behaviors were evoked by tactile stimulation with thin steel needles, and 200 frames per second were recorded using a high-speed camera (HAS-220, Ditect, Tokyo, Japan) mounted on a stereomicroscope (MZ16, Leica, Wetzlar, Germany).

Treated larvae were embedded in O.C.T. compound (Sakura, Tokyo, Japan) and frozen by liquid nitrogen. Frozen blocks were sectioned at 20 μm by a cryostat (CM3050S, Leica). Sequential cryosections were fixed by 4% paraformaldehyde at 25°C for 30 minutes and used for GlyR or α-amino-3-hydroxy-5-methyl-4-isoxazolepropionic acid receptor (AMPA)

immunostaining. Anti-GlyR (mAb4a), antisynapsin1 (106103, rabbit polyclonal IgG, 1:1,000; Synaptic Systems), anti-GluR2/3 (EP929Y, rabbit monoclonal IgG, 1:1,000; Abcam, Cambridge, UK), anti-synaptic vesicle glycoprotein 2A (SV2, mouse IgG₁, 1:200; DSHB, Iowa City, IA), goat antimouse IgG (H + L) (heavy and light) cross-adsorbed secondary antibody Alexa Fluor 488 (A-11001, Thermo Fisher Scientific), goat antimouse IgG (H + L) cross-adsorbed secondary antibody, Alexa Fluor 568 (A-11004, Thermo Fisher Scientific), goat antirabbit IgG (H + L) cross-adsorbed secondary antibody, Alexa Fluor 488 (A-11008, Thermo Fisher Scientific), and goat antirabbit IgG (H + L) cross-adsorbed secondary antibody, Alexa Fluor 568 (A-11011, Thermo Fisher Scientific) were used. NucRed Dead 647 (Thermo Fisher Scientific) was used to stain nuclei of spinal neurons. Fluorescent images of a single plane were captured by a confocal microscope (SP5, Leica). Five fluorescent images were obtained in each larva, and clusters (0.5–2 μm diameter) were quantified using ImageJ³⁰ as described previously.³¹

Statistical Analysis

Statistical significance was tested by unpaired t test. Bar diagrams show mean ± standard error of the mean or as noted otherwise.

Results

Patient Description

Patient 1 (female, 54 years old) had suffered from massive obesity and lymphedema of both legs for many years. She complained of progressive stiffness of the right leg for 6 and of the left leg for 3 months. Repeated falls were reported. Due to both variable stiffness and massive lymphedema, the deep tendon reflexes were difficult to assess, but there were no pathological reflexes. Routine electrophysiology yielded some abnormal synchronization of the blink reflex R2 components considered of unclear significance. The masseter inhibitory reflex, electromyography, evoked potentials, and magnetic-induced evoked potentials gave normal results. Her motility dramatically improved after the first test dose of diazepam (5 mg). Atypical SPS was diagnosed, and in expanded laboratory investigations, she was tested positive for both GAD and GlyR autoantibodies (see Table 1).

Patient 2 (male, 52 years old) had an insidious onset of disease with mainly brainstem and spinal symptoms. He suffered from myoclonic jerks of the trunk and legs, typically precipitated by sudden tactile or acoustic stimuli but also spontaneously. Frequent falls with intact consciousness were reported. He complained of exaggerated startle. The GlyR autoantibody titer was very high in serum and lower in CSF. Gephyrin autoantibodies were also identified (Fig 1A, Table 1).

Patient 3 (male, 63 years old) was operated for cervical spinal stenosis due to progressive spasticity. A few days later, he developed myocloni, seizures, and then the full

clinical picture of PERM. He was respirator-dependent for 5 weeks and recovered slowly under plasma exchange and combined immunosuppressive therapy (see Table 1).

Patient 4 (male, 37 years old) suffered from recurrent lockjaw as the leading symptom, associated with limb stiffness, startle, and unexpected falls.²²

Patient 5 (male, 34 years old) was severely affected and on intensive care and died subsequently. The serum titer of GlyR antibodies was low but definitely positive. The CSF titer was lower compared to the serum titer. The

phenotype did not refer to a full PERM spectrum, but ocular and limb weakness were obvious with myoclonus (see Table 1).

Patient 6 (male, 76 years old) presented with progressive painful muscular rigidity of the lower limbs and myoclonic jerks and later developed impaired consciousness as well as severe autonomic disturbances. High GAD and GlyR autoantibodies were detected in both serum and CSF. He only insufficiently responded to extensive immunotherapy. Artificial ventilation with simultaneous use of

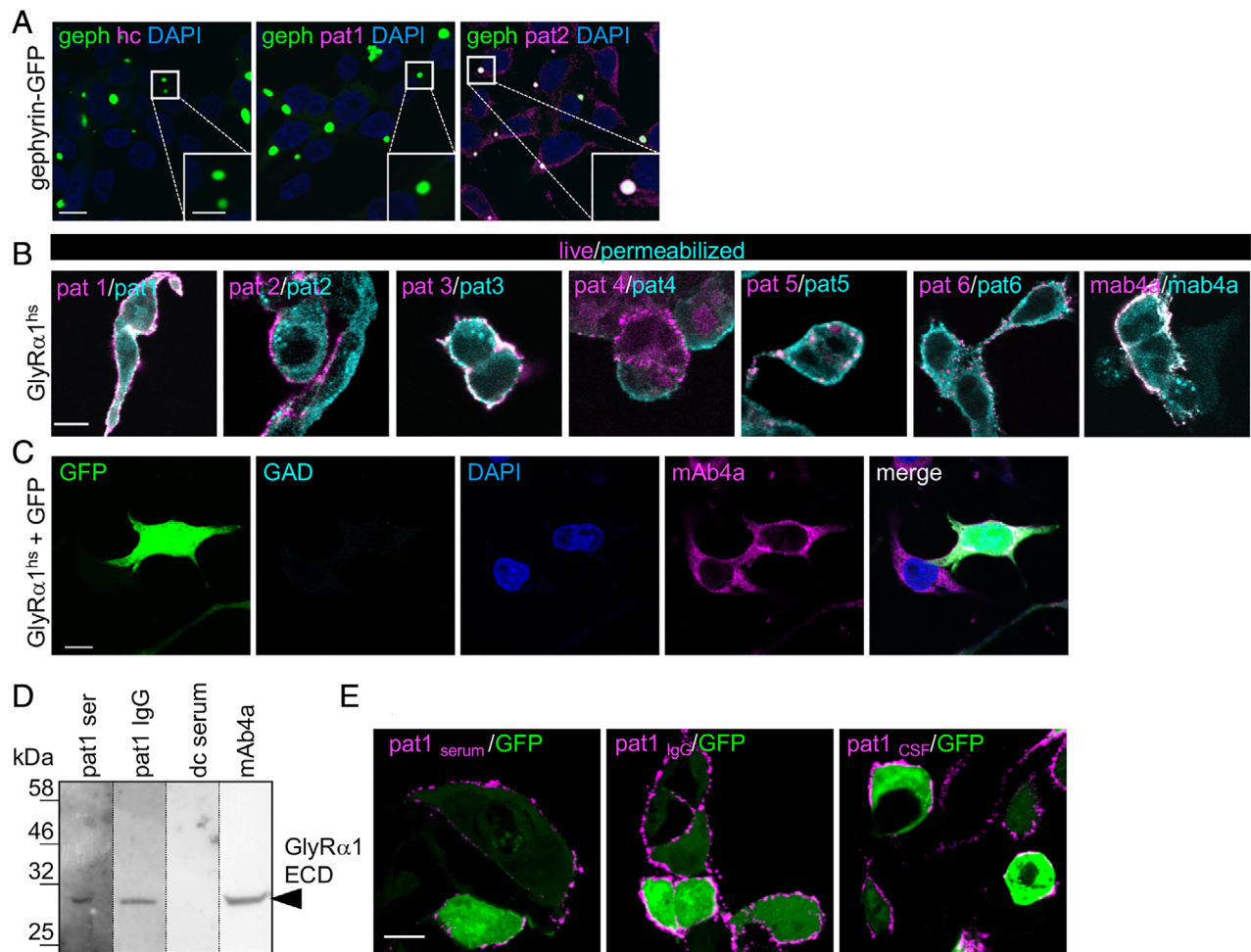


FIGURE 1: GlyR-autoantibodies bind to native and denatured receptor protein. (A) HEK293 cells transfected with a fusion protein of gephrin and green fluorescent protein (geph-GFP, green) were stained with healthy control serum (hc), serum of Patient 1 (pat1), and serum of pat2. Intensive colocalization of targeted gephrin by pat2 autoantibodies and geph-GFP in the GFP blobs within the cell (see magnified inset, white bar in inset represents 5 μ m). Positive gephrin labeling (pink) was also observed in the intracellular part of the cell. Nuclei were marked by 4,6-diamidino-2-phenylindole (DAPI; blue). (B) Transfected HEK293 cells with GlyR α 1^{hs} were used. MAb4a (GlyR α 1^{hs} fixed and permeabilized) was used to detect GlyR α subunits and served as positive control (right image). Serum GlyR-autoantibodies from all patients bind to native (magenta) and denatured (cyan) epitopes of GlyR α 1^{hs}. (C) Cells were transfected with GFP (green) and GlyR α 1^{hs} and stained with glutamic acid decarboxylase (GAD)-positive control serum (cyan) and the pan-GlyR antibody mAb4a (pink). Nuclei were marked by DAPI (blue). Scale bars in A–C represent 10 μ m. (D) The human GlyR α 1 extracellular domain (ECD; residues 1–219 = 30.68kDa) was loaded (10 μ g each lane). The serum of pat1 and the pat1 IgG detected the GlyR α 1 ECD similar to the monoclonal antibody mAb4a (pan-GlyR). dc = disease control, which served as negative control. (E) GlyR α 1^{hs} and GFP cotransfected HEK293 cells were incubated with pat1 serum, pat1 purified IgG, and pat1 cerebrospinal fluid (CSF). Magenta fluorescent signals correspond to GlyR α 1 bound by the antibodies used. Scale bar = 20 μ m.

up to 5 narcotics was needed for several months to control symptoms (see Table 1). Eventually the patient passed away.

GlyR Autoantibodies Bind to the Native but Also to the Denatured GlyR α 1 Receptor Conformation

HEK293 cells transfected with GlyR α 1^{hs} were used for screening of patient sera for GlyR autoantibodies. Following transfection, the GlyR α 1 subunits form homomeric GlyR channels localized at the cellular surface. Double labeling of the GlyR α 1^{hs} receptor first with living (non-fixed, nonpermeabilized) HEK293 cells to explore extracellular binding followed by fixation and permeabilization to detect binding to intracellular localized GlyRs was positive for all patient samples (see Fig 1B, Table 2). Positive staining did not result from presence of coexisting autoantibodies against GAD in serum of pat2 and pat6, because GAD is not expressed in HEK293 cells (see Fig 1C).

To determine whether GlyR autoantibodies bind the ECD (residues 1–219) of the GlyR α 1^{hs}, purified and refolded GlyR α 1^{hs} ECD was analyzed by Western blot. Exemplarily, serum and purified IgG from pat1 were used, and binding to the GlyR α 1^{hs} ECD similar to the monoclonal antibody mAb4a (recognizes residues 96–105 of the mature GlyR) was detectable (see Fig 1D). Hence, cellular and proteinbiochemical analysis revealed strong binding of patient autoantibodies to the receptor in its native

configuration but also binding to intracellular localized GlyR channels.

GlyR autoantibody binding to the native GlyR α 1^{hs} subunit transfected in HEK293 cells was also observed for patient IgG (IgG pat1) following purification from plasma exchange material and patient CSF (see Fig 1E).

GlyR Ion Channel Function Is Altered following Preincubation with Patient Serum

Due to binding of GlyR autoantibodies to the GlyR ECD, autoantibodies might interfere with binding of the neurotransmitter glycine to its orthosteric binding site and/or impair ion channel function. The orthosteric binding site located at the intersubunit interface overlaps with the binding site of the high-affinity antagonist strychnine.¹⁹ Following GlyR-autoantibody binding, radioligand displacement assays showed that neither glycine binding nor strychnine binding was impaired (Fig 2A, B, Table S1). These data argue that the sequence targeted by GlyR autoantibodies differs from the agonist and from the antagonist binding site.

GlyR function was further analyzed using whole-cell current measurements on GlyR α 1^{hs} transfected HEK293 cells following preincubation with patient serum or mAb2b for 1 hour. Specific binding of sera to the transfected cells was verified (see Fig 2C). The time window of 1-hour preincubation with the patient GlyR

TABLE 2. Summary of Binding Capabilities of Patient Samples to Various GlyR Subunits

	Patient 1	Patient 2	Patient 3	Patient 4	Patient 5	Patient 6	Commercial Antibodies	
							mAb2b ^a	mAb4a ^a
Epitope							¹ ARSAPKMSP ¹⁰	⁶ PDLFFANEKG ¹⁰⁵
GlyR α 1 ^{hs}	+	+	+	+	+	+	+	+
GlyR α 1 ^{ch}	+	+	+	+	+	+	+	+
GlyR α 1 ^{dr}	–	+	+	–	–	+	–	+
GlyR α 2 ^{dr}	+	+	+	+	–	–	–	n.d.
GlyR α 3 ^{dr}	–	+	+	+	+	+	–	n.d.
GlyR α 4a ^{dr}	+	+	+	–	–	+	–	n.d.
GlyR α 4b ^{dr}	+/-	+	+	+	–	–	–	n.d.
GlyR β a ^{dr}	+/-	+/-	–	–	–	–	–	n.d.
GlyR β b ^{dr}	–	–	–	–	–	–	–	n.d.

^aLocation of mAb2b and mAb4a epitopes (numbers refer to mature protein) within the sequence; see Figure 4A.

^bChimera contains first 62 amino acid residues of the human α 1 variant and from residue 63 on the sequence of the zebrafish α 1 subunit; proposed epitope of patient autoantibodies is ²⁹ARSAPKMSPSDFLDKLMGRTSGYDARIRPNFKG⁶².

ch = chimeric; dr = *Danio rerio*; hs = *Homo sapiens*; n.d. = not determined.

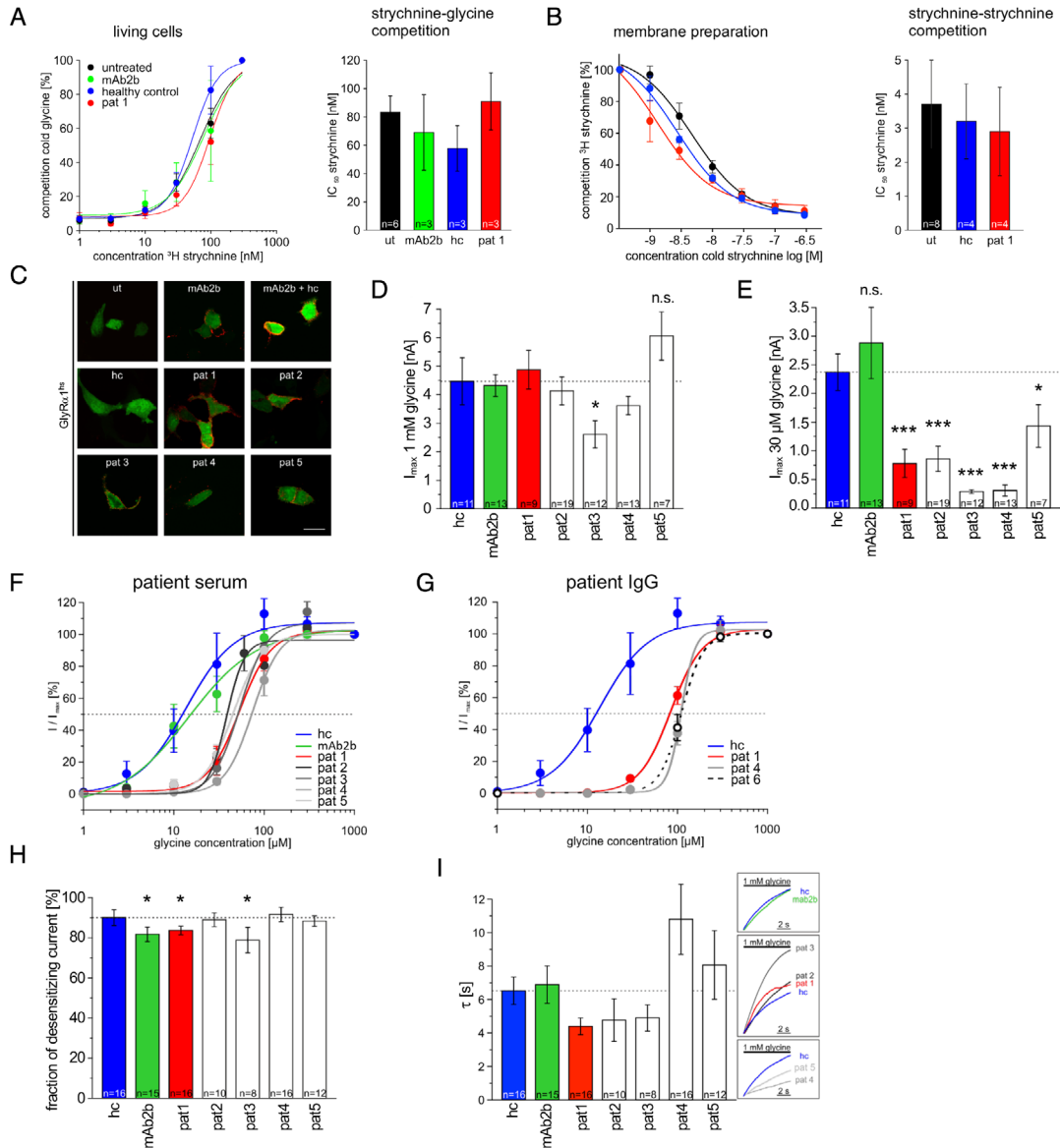


FIGURE 2: Autoantibody binding does not impair glycine binding to the orthosteric glycine binding site but affects glycine potency. Ligand binding was tested using living HEK293 cells (A) and membrane preparations from transfected HEK293 cells with GlyR $^{\text{hs}}$ (B). (A) Living cells were preincubated with mAb2b (green), serum of Patient 1 (pat1; red), or a healthy control (hc; blue) followed by incubation with a saturating concentration of glycine (30mM) and competed with an increasing strychnine concentration series (1, 3, 10, 30, 100, 300nM). Untreated cells were used as control (black). Bar diagram indicates determination of strychnine IC_{50} (nM). (B) Membrane preparations of GlyR $^{\text{hs}}$ transfected cells were used and preincubated with hc or pat1 serum; untreated (ut) membrane preparations served as control. Strychnine–strychnine competition was done using decreasing concentrations of cold strychnine (1,000, 300, 100, 30, 10, 3, 1nM), which were replaced by a fixed strychnine concentration (3nM, ^3H strychnine). Bar diagram indicates quantification of the strychnine IC_{50} values obtained under different preincubation conditions. (C–I) Electrophysiological whole-cell recordings were done from GlyR $^{\text{hs}}$ transfected cells subsequent to 1-hour preincubation of with either hc serum (blue bar), mAb2b (green bar; monoclonal antibody), or different sera from Patients 1–5 (pat1 always shown with red color; white bars refer to other pat2–pat6; various gray colors for pat2–pat6 are used when lines are presented). (C) After recordings were completed, cells were stained with the secondary antihuman IgG Cy3 (except antimouse IgG for mAb2b Cy3) to verify autoantibody binding to transfected cells (magenta signal); green fluorescent protein was cotransfected (green fluorescent signal); untreated cells served as negative control. Green cells were used for whole-cell recordings only. (D) Mean current values evoked by 1mM glycine following 1 hour of treatment with serum from pat1–pat5, with serum from hc (1:10), or with mAb2b (1:500). (E) Currents evoked by 30 μM glycine were significantly reduced after treatment with all patient sera investigated. (F) Dose–response curves for the agonist glycine using a concentration series of 1, 3, 10, 30, 100, 300, and 1,000 μM . Cells were preincubated for 1 hour with either mAb2b or serum from hc or pat1–pat5. Dotted line indicates half-maximal responses (EC_{50}). (G) Dose–response curves (same glycine concentrations as in F) following 1-hour preincubation with purified IgG from pat1 (red line), pat4 (gray line), and pat6 (black dashed line). (H) Fraction of desensitizing currents following an application of the agonist glycine (1mM) for 10 second. (I) Desensitization time constant τ determined over a time period of 10 seconds. The normalized traces (right boxes) illustrate the representative desensitization behavior following incubation with different patient sera as indicated. Dotted lines in D, E and H, I refer to the control measurements with the hc serum. * $p < 0.05$, *** $p < 0.001$. ns = not significant.

autoantibodies is accompanied by an internalization rate of 30% of surface GlyRs (data not shown). A reduction by 30% of cell surface receptors usually does not change maximal current amplitudes as demonstrated by whole-cell recordings from cells transfected with GlyR α 1 mutants associated with hyperekplexia.³² No significant changes in whole-cell maximum currents were found following application of a saturating glycine concentration (1mM; see Fig 2D). Only serum from pat3 caused a significant decrease of glycinergic currents (see Table S1).

Glycine dose–response analysis of the GlyR α 1^{hs} expressed in HEK293 cells revealed an EC₅₀ for glycine around 30 μ M.³³ We used such low glycine concentration to assess whether autoantibodies have an effect on glycine potency. Channel activity provoked by application of 30 μ M glycine was significantly decreased when cells were treated with patient sera compared to serum of a healthy control. In contrast, cells incubated with the monoclonal antibody mAb2b showed no significant change in glycine-evoked currents (see Fig 2E, Table S1).

Recordings of full dose–response curves in the presence of patient sera revealed a 2- to 3-fold decrease in glycine potency compared to a healthy control (see Fig 2F). Glycine EC₅₀ values showed a rightward shift from 26.6 \pm 5.6 μ M obtained from cells incubated with healthy control serum to 45–78 μ M following incubation with patient sera harboring GlyR autoantibodies (see Table S1). From 3 patients, sufficient plasma exchange material was available to purify the IgG (IgG pat1, pat4, and pat6). Interestingly, the preincubation of GlyR α 1^{hs} transfected cells with purified patient IgG fractions resulted in a stronger rightward shift of the EC₅₀ values compared to serum from the same patients (4–5-fold increase in EC₅₀, 105–128 μ M glycine; see Fig 2G, Table S1). To conclude, binding of patient GlyR autoantibodies reduces glycine potency, arguing for a conformational effect of the autoantibodies on ligand binding domain interactions. A higher glycine concentration is required to open the same number of ion channels than in the absence of autoantibodies.

Receptor desensitization is another ion channel property characterizing ion channel closure in the presence of neurotransmitter. We found small changes in receptor desensitization in the presence of glycine following preincubation with patient serum for 1 hour. The fraction of the desensitizing currents decreased significantly following incubation with pat1 or pat3 serum compared to healthy control (see Fig 2H). A comparison of the decay time constant τ following incubation with pat1 and pat3 sera revealed a tendency toward faster ion channel transition into the desensitized stage compared to healthy control serum (see Fig 2I, Table S1). These data demonstrate that at least a certain fraction of channels close faster upon

preincubation with GlyR autoantibodies in the presence of neurotransmitter than in the absence of autoantibodies. Furthermore, a small receptor fraction stayed in the open state until glycine was washed off. Interestingly, pat4 and pat5 sera had no influence on the fraction of desensitizing current of the GlyRs compared to healthy control serum (see Fig 2H, I, Table S1). The monoclonal antibody mAb2b (green bars) was used in all experiments to determine whether any observed effect is due to a general binding of antibodies to the GlyR ECD, for example, binding of mAb2b to the GlyR α 1 also decreases the fraction of desensitized currents. Hence, GlyR autoantibody binding seems to affect structural transitions of the receptor between the open and the desensitized state.

Patient Antibodies and a Commercially Available Monoclonal Antibody Colocalize to the GlyR α 1 Subunit but Do Not Compete for the Same Binding Site

GlyR α 1^{hs} expressed in HEK293 cells was specifically stained with autoantibody-containing serum from patients. These stains colocalized with the signal obtained following mAb2b (binds to extracellular located residues 1–10 of the mature protein) incubation, a specific GlyR α 1 antibody (Fig 3). Competition analyses of pat1 serum and mAb2b were performed to identify possible replacements or epitope differences of both antibodies. Simultaneous incubation of HEK293 cells with pat1 serum and mAb2b (1:50) as well as successive incubation yielded intense colocalization of both signals. Using mAb2b concentrations of 1:100, 1:500, and 1:1,000, and 1:2,000 resulted in similar staining patterns. The experiments were performed under saturating conditions proven by sequential labeling of fixed/nonpermeabilized cells with the same antibody twice (1 hour primary antibody either serum pat1 1:50 or mAb2b 1:500 followed by secondary antibody incubation with goat antihuman Cy3, then again 1 hour primary either serum pat1 or mAb2b labeled with another secondary antibody coupled to Alexa Fluor 488). Following the second incubation round, no staining of the secondary antibody coupled to Alexa Fluor 488 was detectable. In sum, both the patient autoantibodies and the commercial antibody mAb2b are able to bind simultaneously to the human GlyR and do not compete for the same binding site.

The N-Terminus of GlyR α 1^{hs} Represents a Common Autoantibody Epitope

Because GlyR autoantibodies bind nonfixed living cells that express GlyR α 1^{hs} as well as to the purified ECD, the GlyR ECD represents a target sequence of GlyR autoantibodies (Fig 4). GlyR α subunits are highly homologous

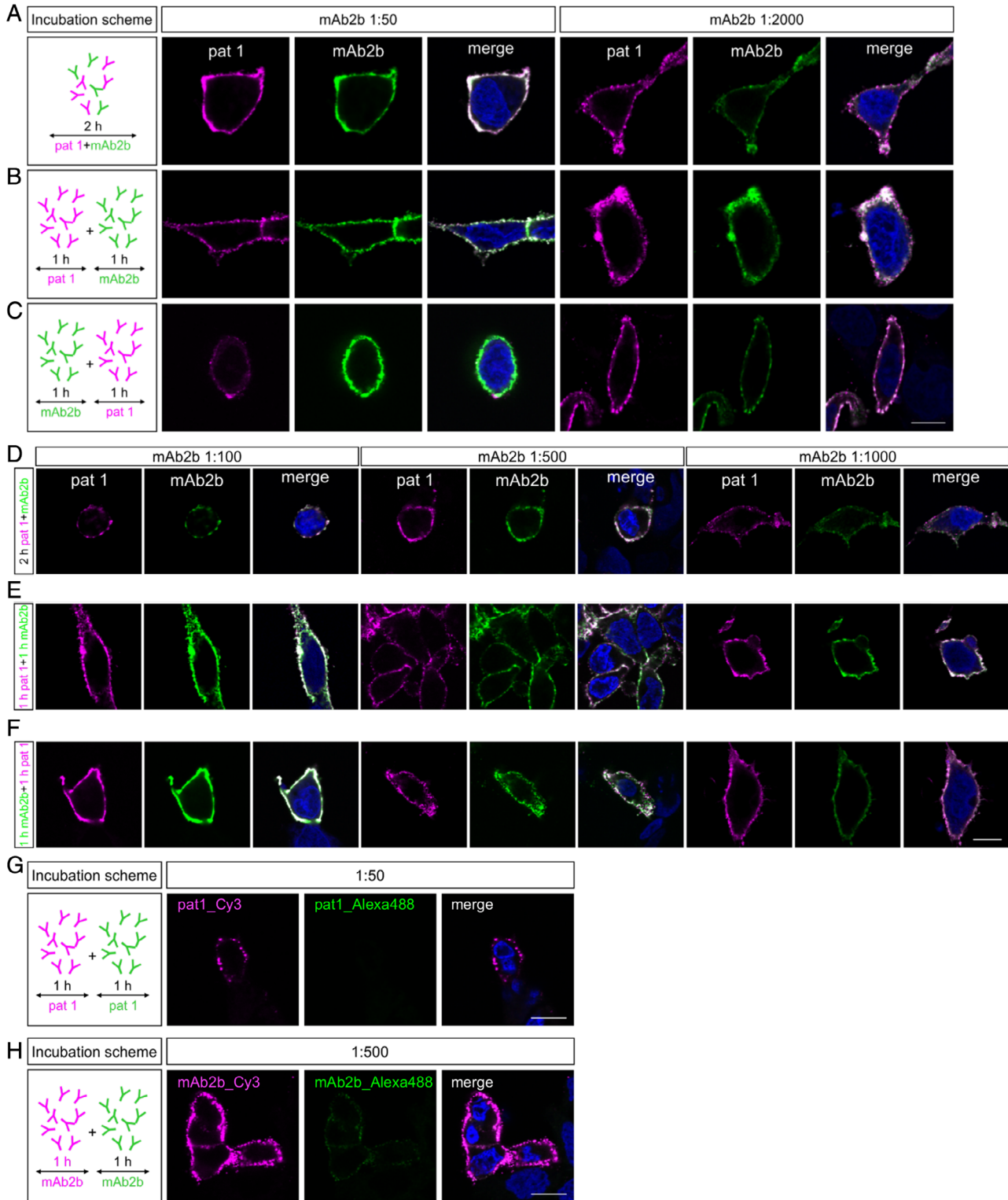


FIGURE 3: Patient serum does not compete with mAb2b for the same binding sites at the human GlyR α 1 subunit. (A–C) Left images: Incubation schemes of Patient 1 (pat1) serum and mAb2b incubated either together for 2 hours with pat1 serum (1:50) and mAb2b (1:50) using 3 different protocols. (A–C) Middle images: Fluorescence signals of GlyR α 1^{hs} transfected HEK293 cells incubated with pat1 serum (1:50) and mAb2b (1:50) using 3 different protocols. (A–C) Right images: Different antibody concentrations were used (pat1 serum 1:50 and mAb2b 1:2,000). (D–F) Fluorescence signals of GlyR α 1^{hs} transfected HEK293 cells incubated with pat1 serum (1:50) and mAb2b (1:100; 1:500; 1:1,000) together for 2 hours (D), successively first with pat1 serum for 1 hour followed by 1 hour with mAb2b (E), and successively first 1 hour with mAb2b followed by pat1 serum for 1 hour (F). (G) Cells were incubated with pat1 serum 1:50 twice. Following the first pat1 incubation, labeled protein was stained with secondary goat antihuman Cy3 (left). Pat1 serum was applied again for 1 hour and stained with goat antihuman Alexa Fluor 488 (middle). (H) Cells were incubated with mAb2b 1:500 followed by secondary staining with goat antimouse Cy3. mAb2b was applied again for 1 hour and stained with goat antimouse Alexa Fluor 488. Scale bars = 10 μ m.

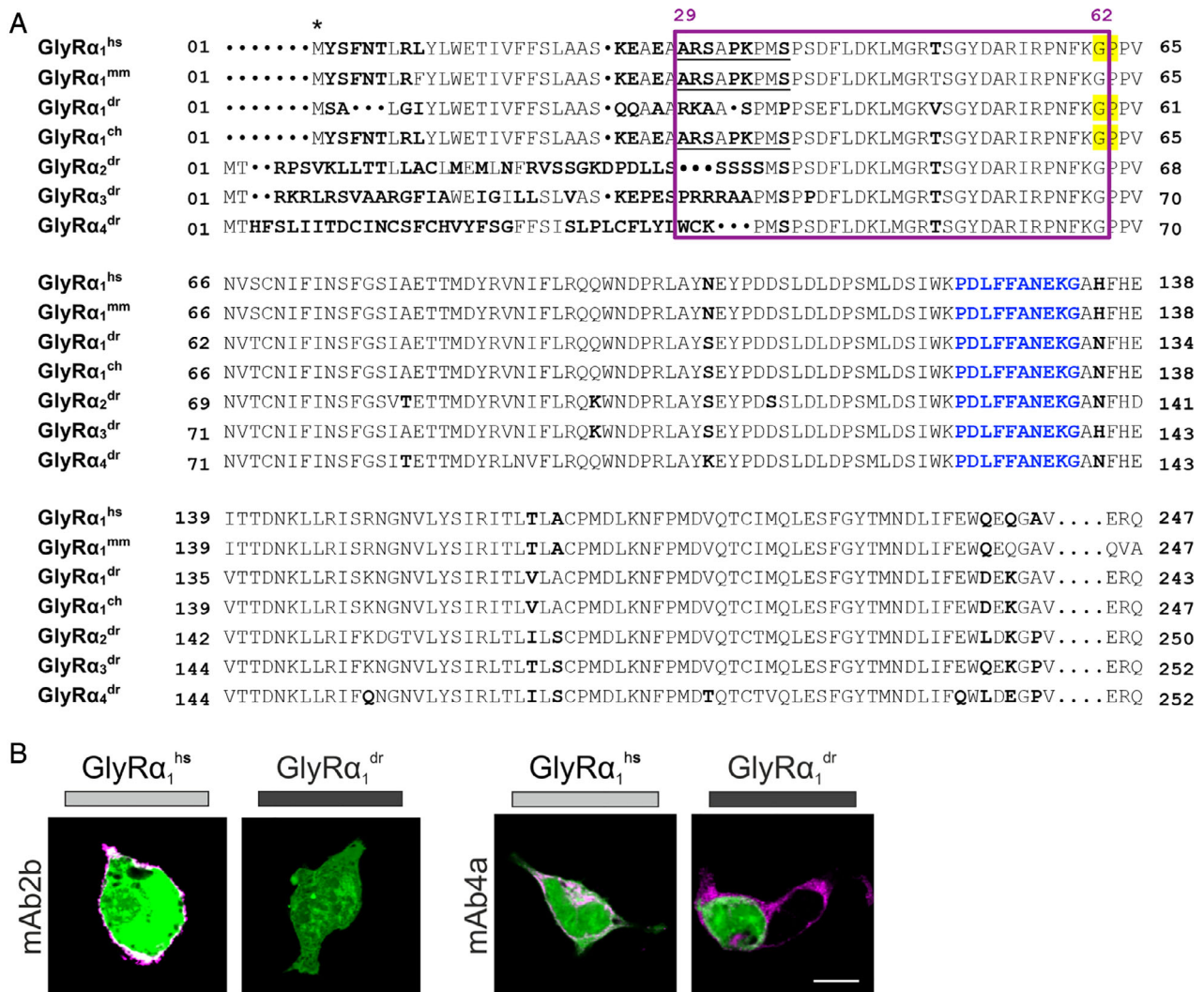


FIGURE 4: The far GlyR N-terminus determines species specificity of GlyR autoantibodies. (A) Amino acid sequence alignment of the extracellular domains of the immature GlyR α_1^{hs} , GlyR α_1^{mm} , GlyR α_1^{dr} , GlyR α_1^{ch} , GlyR α_2^{dr} , GlyR α_3^{dr} , and GlyR α_4^{dr} . Deviations in amino acid alignment are displayed in bold letters. The epitope of the monoclonal antibody mAb2b (α_1 -specific antibody recognizing residues 1–10 of the mature protein) is underlined; the epitope of mAb4a pan-GlyR antibody (present in GlyR α_1^{dr} , GlyR α_1^{hs} and GlyR α_1^{ch} residues 96–105) is marked by blue letters. Start of protein is marked by an asterisk (signal peptide first 28 residues). Residues that refer to the site of the restriction enzyme PpuM I used to generate a chimera are shaded in yellow. The proposed epitope of GlyR autoantibodies is marked by a pink box. (B) HEK293 cells where cotransfected with green fluorescent protein (green) and GlyR α_1^{dr} . The mAb2b antibody binds only to GlyR α_1^{hs} but not to GlyR α_1^{dr} , whereas the pan-GlyR antibody mAb4a binds both the human and the zebrafish α_1 subunit. White bar = 10 μ m. ch = chimeric; dr = *Danio rerio*; hs = *Homo sapiens*; mm = *Mus musculus*.

in the overall ECDs among species, but sequence differences exist at the far N-terminal part. The epitope of the mAb2b antibody (residues 1–10 of the mature protein ¹ARSAPKPMSP¹⁰) is present in human and mouse (*Mus musculus*) but is not present in *D. rerio*, explaining non-binding of the specific GlyR α_1 antibody mAb2b (see Fig 4, Table 2). In contrast, the mAb4a binding site to residues 96 to 105 (mature protein) is identical between zebrafish and human GlyR α_1 and was used as a positive control. To investigate whether the far N-terminal part is at least partially involved in autoantibody binding, a

chimeric GlyR α_1 construct (GlyR α_1^{ch}) was generated with an exchange of the N-terminal region (residues ¹M–⁶²G) harboring pronounced differences in GlyR α_1^{hs} and GlyR α_1^{dr} (Fig 5). Due to presence of the mAb4a epitope in GlyR α_1^{ch} , mAb4a stained the chimeric construct. MAb2b, unable to recognize GlyR α_1^{dr} , showed detection of GlyR α_1^{ch} due to the presence of the first 62 residues of the human sequence. Serum from pat1, pat3, pat4, and pat5, but not pat2 and pat6 resembled the mAb2b recognition pattern (see Fig 5C, Table 2). Residues 1 to 28 refer to the signal peptide of the GlyR and

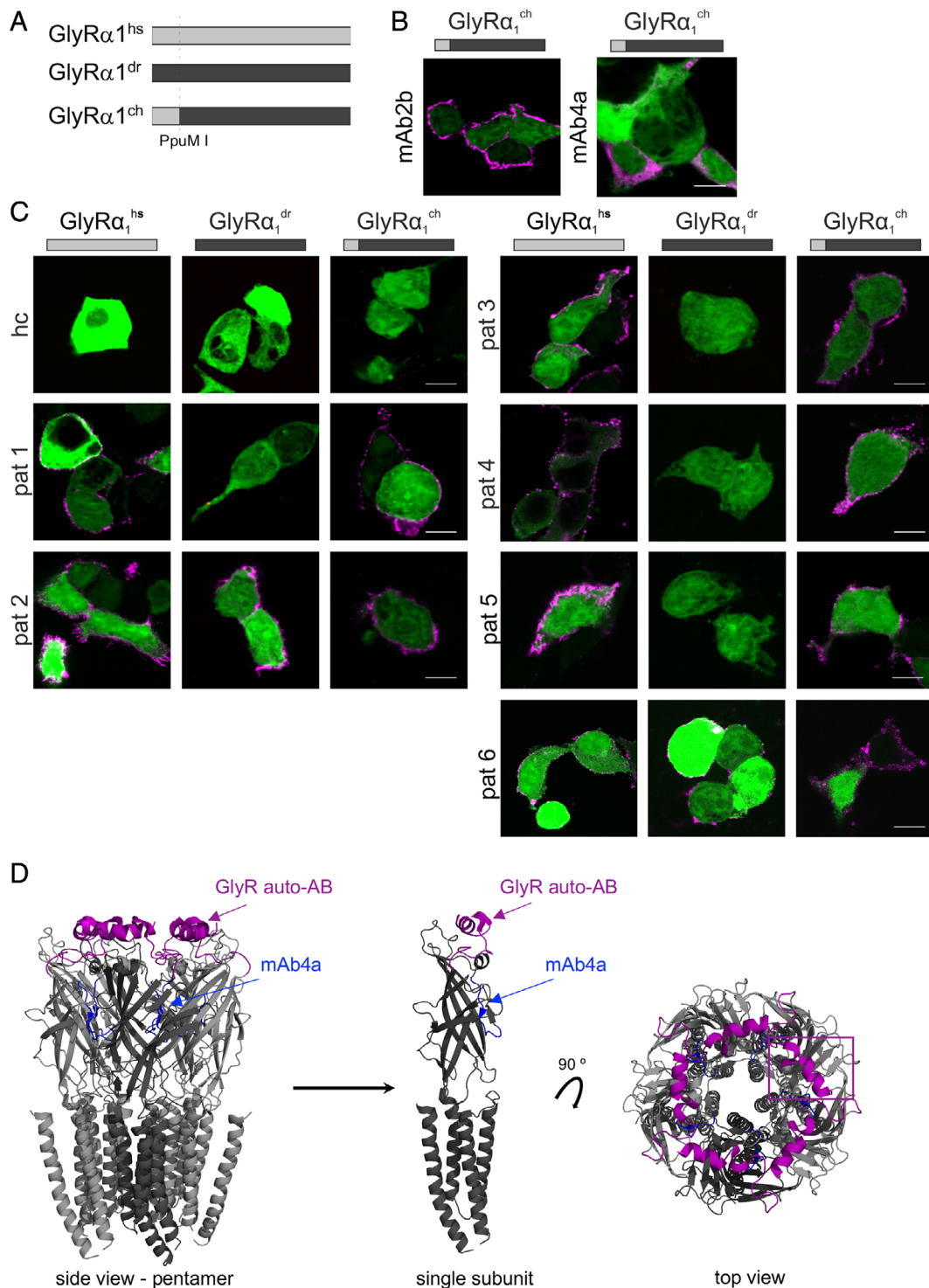


FIGURE 5: The GlyR α_1 far N-terminus represents a common epitope for GlyR autoantibodies. (A) Chimeric GlyR α_1^{ch} is composed of the N-terminal part of GlyR α_1^{hs} (gray bar) and the C-terminal part of GlyR α_1^{dr} (black bar). Cutting site is indicated by a vertical dotted line (PpuM I, Fig 4A). (B) HEK293 cells where cotransfected with green fluorescent protein (green) and either GlyR α_1^{hs} , GlyR α_1^{dr} , or GlyR α_1^{ch} . GlyR α_1^{ch} was detected by the pan-GlyR antibody mAb4a and mAb2b. (C) Serum of Patient 1 (pat1), pat3, pat4, and pat5 refer to the same staining pattern as mAb2b. The serum from pat2 and pat6 stained all 3 GlyR variants: GlyR α_1^{hs} , GlyR α_1^{dr} , and GlyR α_1^{ch} . Serum from a healthy control served as negative control. White bars = 10 μ m. (D) Structural model of the GlyR α_1 according to Du et al.¹⁹ Labeled are the proposed epitope for GlyR autoantibodies (pink) and the mAb4a epitope (blue). Left, pentamer; center, single subunit from side; right, top view on pentamer GlyR. Note the surface localization of the GlyR autoantibody epitope (pink) in contrast to the mAb4a epitope (blue) deeper in the structure at the interface between two adjacent subunits. ch = chimeric; dr = *Danio rerio*; hs = *Homo sapiens*.

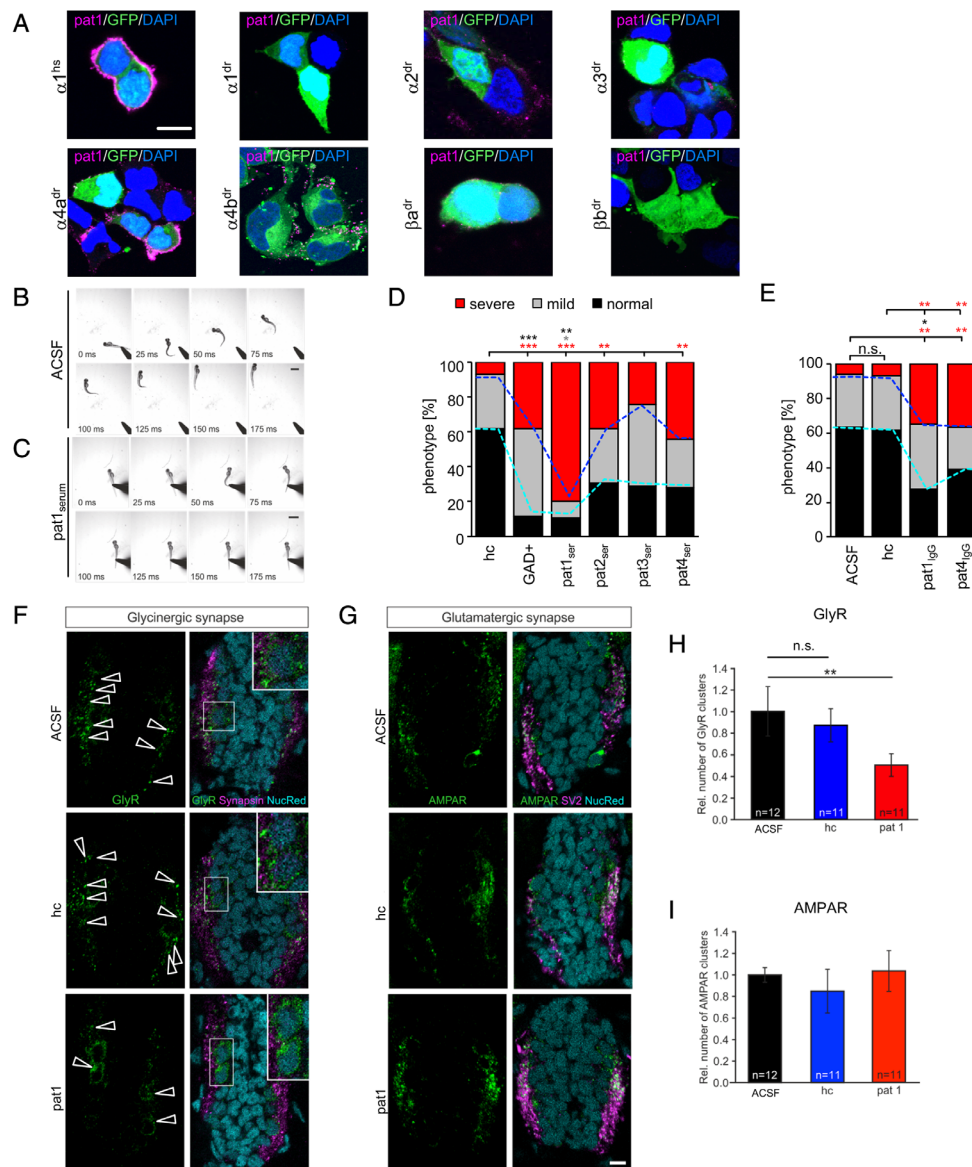


FIGURE 6: Zebrafish larvae show abnormal escape response and reduced spinal cord GlyR cluster numbers upon treatment with patient serum. (A) Transfected HEK293 cells with various GlyR subunits of the zebrafish (*dr = Danio rerio*; $\alpha 1$, $\alpha 2$, $\alpha 3$, $\alpha 4a$, $\alpha 4b$, βa , βb) stained with serum of Patient 1 (pat1; magenta). Green fluorescent protein (GFP; green) was cotransfected. 4,6-Diamidino-2-phenylindole (DAPI) was used to stain the nuclei. Note that pat1 serum specifically targets GlyR $\alpha 2$ and $\alpha 4a$ (magenta). To some extent, $\alpha 4b$ and βa were also stained. White bar = 20 μ m. (B, C) Sequence photographs of escape responses to tactile stimulation. The tip of the steel needle is visible in the bottom corner of each image. Touching the larva is indicated as 0 milliseconds. (B) Escape response of a healthy control (hc) serum permeated larva ($n = 42$). ACSF = artificial cerebrospinal fluid. (C) Escape response of a pat1 serum permeated larva ($n = 29$). This larva showed a weak convulsion in response to stimulation and remained stiff instead of initiating swimming. Scale bars = 1mm. (D, E) Stacked bar diagrams representing the different conditions of permeated larvae with patient serum or patient IgG. Black bars refer to portion of normal escape response (see also cyan dotted line for differences between conditions), gray bars refer to mild affected escape response, and red bars refer to severe impaired escape behavior (see also blue dotted line). All values are given as percentages. Animals analyzed for control conditions were ACSF, $n = 38$; hc, $n = 42$; glutamic acid decarboxylase (GAD)⁺, $n = 34$; pat1, $n = 29$; pat2, $n = 29$; pat3, $n = 45$; pat4, $n = 32$; pat1 IgG, $n = 43$; pat4 IgG, $n = 36$. * $p < 0.05$, ** $p < 0.01$, *** $p < 0.001$. (F) Immunostaining of glycinergic synapses (GlyR green). Antisynapsin1 antibody was used as primary antibody to detect presynaptic terminals (magenta); NucRed is shown in blue. Boxed areas in F are enlarged at the top right corners of the images showing staining in close proximity to the nucleus. (G) Immunostaining of glutamatergic synapses. Antisynaptic vesicle glycoprotein 2A (SV2) antibody was used as primary antibody to detect presynaptic terminals (magenta). α -Amino-3-hydroxy-5-methyl-4-isoxazolepropionic acid receptors (AMPA) were stained with anti-GluR2/3 antibody (green) and DAPI (blue). Scale bar = 5 μ m. (H, I) Relative number of GlyR clusters and AMPAR clusters following injection of the zebrafish with hc (blue) or pat1 serum (red) as compared to ACSF controls (black columns). ** $p < 0.01$. ns = not significant.

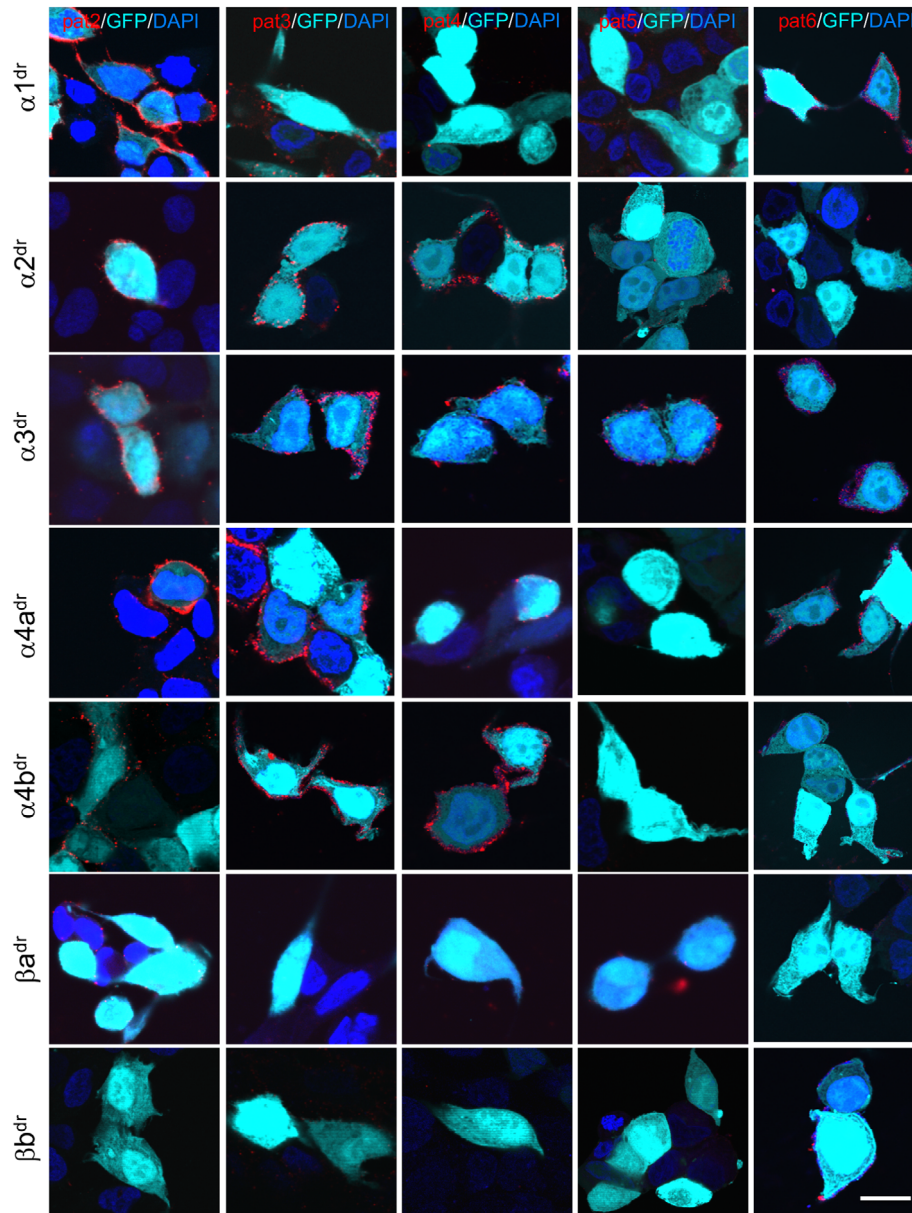


FIGURE 7: All patient sera target some GlyR subunits of the zebrafish. HEK293 cells cotransfected with green fluorescent protein (GFP; cyan) and GlyR subunits of *Danio rerio* (dr; $\alpha 1$, $\alpha 2$, $\alpha 3$, $\alpha 4a$, $\alpha 4b$, βa and βb) were stained with sera from Patient 2 (pat2), pat3, pat4, pat5, and pat6 (red). 4,6-Diamidino-2-phenylindole (DAPI) (blue) labeled the nucleus. White bar in right column represents 20 μ m. Note that most patient sera target $\alpha 2$, $\alpha 3$, and $\alpha 4a$. The β subunits of *D. rerio* do not represent a common target for the human GlyR autoantibodies. Stainings for the β subunits were performed following permeabilization of the cells, because the β subunits are not transported to the surface without the presence of α subunits.

are therefore not present in the mature surface localized receptor, arguing for the identification of a common epitope of GlyR autoantibodies with residues A²⁹ to G⁶² (see Fig 4A). At the structural level, A²⁹-G⁶² refers to the first α -helical element at the far N-terminus of GlyR $\alpha 1$. This region represents an important allosteric binding site in GlyRs and in nAChR.^{21,34} In contrast to the mAb4a epitope (blue), the region A²⁹-G⁶² (pink) is localized at the surface of the protein and thus easily accessible by GlyR autoantibodies (see Fig 5D).

Impaired Escape Behavior in Zebrafish Larvae following Administration of Patient Serum

Our in vitro experiments showed that autoantibodies themselves are probable agents in the pathogenesis of SPS spectrum disorders.

To verify the pathogenic potential of autoantibodies in vivo,¹² we used the passive transfer of autoantibodies in the zebrafish model. The touch-evoked escape response in zebrafish mirrors the startle phenotype in human and mice. A normal escape response consists of escape

contractions with typically 2 to 3 rapid alternating contractions of the axial muscles.^{35–37} Our epitope screen showed no staining of GlyR α 1^{dr} by pat1 serum. The analysis of binding of other zebrafish GlyRs as a precondition for the *in vivo* transfer revealed targeting of pat1 serum for α 2^{dr}, α 4a^{dr}, and marginally α 4b^{dr} and β a^{dr}, respectively (Fig 6A, Table 2). Patient sera 2 to 6 exhibited staining of some of the α subunits from zebrafish (pat2: α 1^{dr}, α 2^{dr}, α 3^{dr}, α 4a^{dr}, α 4b^{dr}, β a^{dr}; pat3: α 1^{dr}, α 2^{dr}, α 3^{dr}, α 4a^{dr}, α 4b^{dr}; pat4: α 2^{dr}, α 3^{dr}, α 4b^{dr}; pat5: α 3^{dr}; pat6: α 1^{dr}, α 3^{dr}, α 4a^{dr}, α 4b^{dr}; Fig 7, Table 2).

A lesion of the skin covering the 4th ventricle of zebrafish larvae permitted diffusion of autoantibodies into the intraventricular space. Wild-type larvae at 72 hpf normally respond to a tactile stimulus with a rapid initiation of an escape movement. Pretreatment (ACSF) and healthy control serum permeated larvae showed mainly the expected escape response within a time window of 175 milliseconds (see Fig 6, Video S1). Severely impaired escape responses with failure to initiate swimming in pat1 serum permeated larvae were observed (Video S2). Three types of escape behavior were compared (normal: turn and subsequent swimming; mild: abnormal escape behavior with a dorsal bend followed by swimming of <2cm; and severe: a dorsal bend without escape swimming). All sera treated larvae showed a significantly increased fraction of the severe escape phenotype compared to ACSF and healthy control serum permeated larvae (Table S2). Hence, the portion of normal escape response was decreased compared to ACSF and healthy control treated larvae. A serum positive for GAD autoantibodies served as a control, because (1) pat1 carried GlyR and GAD⁺ autoantibodies and (2) GAD autoantibodies have also been associated with SPS. The presence of GAD⁺ autoantibodies also impaired the escape response in the treated larvae. The effect was, however, more pronounced in pat1, carrying both GlyR and GAD autoantibodies. Similarly, the purified IgG from pat1 and pat4 significantly increased the severity of the escape response (see Fig 6E, Table S2). Our data clearly demonstrate the pathologic potential of GlyR autoantibodies generating a motor phenotype in the affected animals.

Patient Serum Significantly Decreases GlyR Clusters in Zebrafish Larvae

To assess whether lower GlyR numbers account for the GlyR pathomechanism in the *in vivo* situation and thus interfere with swimming initiation, GlyR internalization was investigated. The number of GlyR clusters in the lateral region of the spinal cord was significantly reduced in pat1 serum permeated larvae compared to untreated larvae (see Fig 6F, H). In some fluorescent images,

immunostaining signals of GlyR were observed around the cellular nucleus (see enlarged inset in Fig 6F). To control for autoantibody and patient serum specificity, the numbers of excitatory AMPAR clusters were also quantified but showed no differences upon GlyR autoantibody injection (see Fig 6G, I). These results suggest that autoantibodies to GlyRs in the patient serum facilitate the internalization of GlyR and induce motor dysfunction as a consequence thereof. We cannot, however, rule out the possibility that the access of the mAb4a epitope is masked by the presence of the autoantibodies.

Discussion

GlyR autoantibodies have been associated with 2 characteristic neurological syndromes, SPS and PERM.^{4,5,7,38,39} The present paper expands the current knowledge on the pathology of GlyR autoantibodies by (1) demonstrating impaired GlyR functionality in the presence of autoantibodies, (2) identifying a common GlyR autoantibody epitope in the N-terminus of the receptor, and (3) inducing an obvious motor phenotype following an *in vivo* passive transfer of GlyR autoantibodies into the zebrafish.

SPS patient phenotypes are variable; for example, patients largely differ in antibody titer, age at onset, responsiveness to treatment, and relapse occurrence.⁴ In some patients harboring GlyR autoantibodies, the disorder is associated with tumors, others additionally suffer from epilepsy, others develop autoantibodies as primary disease.^{40–43} A recent publication identified mainly IgG1 within patient sera harboring GlyR autoantibodies and showed complement activation.⁴ Furthermore, receptor internalization subsequent to receptor cross-linking and impaired GlyR function has been suggested as a potential disease mechanism.¹⁴

To identify a binding epitope for GlyR autoantibodies, we first demonstrated that GlyR autoantibodies bind to various human and zebrafish GlyR α subunits, arguing for an epitope common to all α subunits. Binding to an extracellular portion of human α 1, α 2, α 3 GlyR subunits has also been shown previously.^{4,22} The specific GlyR immunoreaction in transfected living cells and to the purified GlyR ECD protein argues for an accessible epitope of the GlyR autoantibodies in the extracellular receptor domain (residues 1–219). A further hint to the extracellular autoantibody epitope was derived from stainings of the zebrafish GlyR α 1^{dr} protein. Although highly homologous in most parts of the ECD, the zebrafish GlyR α 1 protein varies largely at the far N-terminus compared to the human α 1. Serum from pat1, pat3, pat4, and pat5 did not bind zebrafish GlyR α 1^{dr}. Humanization of the zebrafish variant by transferring residues 1 to

62 restored binding. Residues 1 to 28 refer to the signal peptide of the receptor and are thus not present in the mature protein, arguing that residues ²⁹A to ⁶²G in the N-terminal part of the human GlyR α 1 subunit represent a common epitope for GlyR autoantibodies. The first 10 residues of the mature GlyR constitute the binding epitope of the GlyR α 1-specific monoclonal antibody mAb2b (²⁹A–³⁸P in nonmature protein). The competition experiment with the human GlyR autoantibodies and mAb2b revealed labeling with both antibodies, thus arguing for a lack of competition between each other. Therefore, the previously suggested binding of GlyR autoantibodies to the extracellular receptor domain⁴ can be further curtailed to residues ²⁹A to ⁶²G overlapping but not identical with the mAb2b epitope.

Recently, functional changes of the glycine receptor expressed in spinal cord motoneurons upon preincubation with GlyR autoantibodies have been shown.¹⁴ The mechanism is, however, not completely understood. For N-methyl-D-aspartate receptor autoantibodies, a direct functional inhibition as a consequence of autoantibody binding has been reported.⁴⁴ Functional alterations of the GlyR have been proposed to result from GlyR cross-linking and subsequent internalization but also from a direct antagonistic action on GlyRs.^{4,14} One-hour incubation with the GlyR autoantibody resulted in receptor internalization of about 30 to 50%.⁴ Current knowledge from GlyR α 1 mutant receptors associated with hyperkplexia³² revealed that a reduction by 30 to 50% of cell surface receptor protein does usually not change maximal current amplitudes. If, however, the GlyR protein is reduced by >85%, a decrease in glycine-gated chloride current amplitudes at maximal glycine concentrations would be expected.^{33,45,46} Our results show that pretreatment of GlyRs with patient autoantibodies had no significant influence on glycinergic currents at saturating glycine concentrations, thus arguing for no impact of GlyR autoantibodies on glycine efficacy. In contrast, increased glycine EC₅₀ values determined for all 6 patient sera suggest a general effect of GlyR autoantibodies on glycine potency. Thus, a higher glycine concentration is required to open the same number of channels as in the absence of autoantibodies. Similar changes on glycine potency have been observed for GlyR α 1 subunit mutants associated with human hyperkplexia, resulting in massive muscle stiffness and tremor.^{33,47–49} Hence, the functional alteration of inhibitory neurotransmission is most probably due to direct binding of GlyR autoantibodies and possibly conformational blocking of the Cl⁻ channel. GlyR autoantibodies are unable to displace the agonist glycine or the antagonist strychnine from their orthosteric binding sites. Conformational blocking of GlyRs may therefore

influence structural transitions between open/closed and desensitized stages and thus underlie GlyR autoantibody pathology.

We further observed changes in the decay time constants, arguing that the time the channel spends in its open conformation is affected by autoantibody binding. Moreover, GlyR function was also affected by changes in the fractions of desensitized channels. GlyR channels with altered desensitization as well as differences in the kinetics of channel closure have also been reported to underlie the neuromotor phenotype in patients harboring genetic GlyR variants and suffering from human hyperkplexia.^{49,50} These GlyR mutations lead to structural changes and thus differences in the chemical bond formations to other residues within the structure. From X-ray crystallography and cryoelectron microscopy, the GlyR structure is known in its open, closed, and desensitized stages.^{19–21} At the structural level, the identified common GlyR autoantibody epitope ²⁹A to ⁶²G refers to the α 1-helical part in the far N-terminus and the loop between α 1-helix and the first β -sheet β 1. Interestingly, residues within pre- β 1 (R⁵⁷ and F⁶⁰) were determined to directly interact with the allosteric analgesic potentiator AM3607. The GlyR α 3 bound to glycine and AM3607 was suggested to represent the desensitized form of the receptor.²¹ Thus, binding of GlyR autoantibodies to the same pre- β 1 region in the GlyR ECD might explain their influence on receptor desensitization. Moreover, the α 1-helix changes its positions between the open, closed, and desensitized stages.¹⁹ Binding of GlyR autoantibodies to the α 1-helix possibly additionally hinders transitions between different ion channel configurations and hence slows down inhibitory neurotransmission in the patients.

The pathogenicity of GlyR autoantibodies was further confirmed by transfer experiments of autoantibodies into zebrafish larvae, leading to impaired escape responses and reduction of synaptic GlyR clusters in the spinal cord. The escape behavior in zebrafish is affected if glycinergic inhibition is disrupted either by mutations of GlyR subunits^{51–53} or by the DEAH-box RNA helicase that controls GlyR expression.³⁶ Due to a mutation in the GlyR, the impairment of the nerve–muscle circuit results in muscle stiffness, disabling the zebrafish so that it cannot swim away from a tactile stimulus. Instead, following 1 or 2 turns, the zebrafish subsequently stops (severe phenotype). Thus, a similar impaired escape response was assumed after GlyR autoantibody binding to the receptor targets in the zebrafish larvae. Such phenotypic readout in the zebrafish reflects the neuromotor syndromes in patients with anti-GlyR autoantibodies associated with SPS characterized by muscle stiffness and an exaggerated startle response upon tactile or acoustic stimuli. We showed a significant increase in the severity of escape response impairment using serum or purified IgG

from human patients. The response was, however, not an all or none response, presumably due to compensation by other GlyR subunits. A further limitation of this analysis was the fraction of larvae exhibiting a severe or intermediate phenotype due to the lesion that has been set to allow the autoantibodies to find their targets even when subjected to ACSF or control sera injection. The concomitantly reduced GlyR clusters in zebrafish larvae suggest internalized GlyR α 1 receptors upon autoantibody binding or steric hindrance of the pan-GlyR antibody to reach its epitope upon binding of GlyR autoantibodies to the GlyR α N-terminal domain. The remaining staining following incubation with patients' GlyR autoantibodies suggests binding of the pan-GlyR antibody to other GlyR subunits of the zebrafish (α 2, α 3, α 4, and β). The reduced GlyR cluster number upon autoantibody binding is in line with receptor cross-linking and internalization of GlyRs shown previously.⁴ Moreover, reduced synaptic localization of GlyRs also underlies severe neuromotor phenotypes in genetic GlyR variants as demonstrated in the shaky mouse model.²⁹

In conclusion, we show that GlyR autoantibodies lead to functional disruption of glycine-gated Cl⁻ channels with main impact on glycine potency. Therefore, in vivo higher glycine concentrations are required to activate the same number of GlyR channels as in the absence of GlyR autoantibodies. The demonstrated functional impairment of novel synthesized and membrane-incorporated receptor protein significantly contributes to disease progression in addition to receptor internalization. Furthermore, our data argue that GlyR autoantibodies are a direct cause of the disease, because the transfer of human GlyR autoantibodies to zebrafish larvae generated impaired escape behavior in the animal model compatible with the enhanced startle response in human beings. Considering future perspectives, one might think of autoantibody binding by soluble extracellular GlyR α 1 protein, which may help to neutralize autoantibodies in the serum⁵⁴ and thus prevent disease relapses more specifically.

Acknowledgment

This work was supported by the German Research Foundation SO328/9-1 (C.S.), VI586/8-1 (C.V.), and GE2519/8-1 (C.G.), research unit SYNABS FOR3004, Grant-in-Aid for Scientific Research on Innovative Areas 17H05578 from the Japan Society for the Promotion of Science (H.H.), the Naito Foundation (H.H.), and the Japan Epilepsy Research Foundation (H.H.). The work of C.J.K. was funded by EU FP7 Neurocypres. N.v.W. and V.R. are supported by the Würzburg Graduate School of Life Sciences.

We thank Dr A. Vincent for providing pat5 serum for this study; Dr C. Probst, S. Mindorf, and I. Dettmann from the Institute for Experimental Immunology, Euroimmun, Lübeck, Germany for the determination of the GAD titers of the patient sera; G. Schell and N. Vornberger for excellent technical assistance; and S. Hengst, Rudolf Virchow Center for Experimental Biomedicine, for assistance with the scintillation counting.

Author Contributions

C.S., C.J.K., and C.V. contributed to conception and design of the study. Acquisition and analysis of data were done by all authors. Drafting the text and preparing the figures were done by V.R., N.v.W., K.O., H.H., N.S., J. W., C.G., and C.V.

Potential Conflicts of Interest

Nothing to report.

References

- Ameli R, Snow J, Rakocevic G, Dalakas MC. A neuropsychological assessment of phobias in patients with stiff person syndrome. *Neurology* 2005;64:1961–1963.
- Balint B, Bhatia KP. Stiff person syndrome and other immune-mediated movement disorders—new insights. *Curr Opin Neurol* 2016;29:496–506.
- Henningsen P, Meinck HM. Specific phobia is a frequent non-motor feature in stiff man syndrome. *J Neurol Neurosurg Psychiatry* 2003;74:462–465.
- Carvajal-Gonzalez A, Leite MI, Waters P, et al. Glycine receptor antibodies in PERM and related syndromes: characteristics, clinical features and outcomes. *Brain* 2014;137(pt 8):2178–2192.
- Hutchinson M, Waters P, McHugh J, et al. Progressive encephalomyelitis, rigidity, and myoclonus: a novel glycine receptor antibody. *Neurology* 2008;71:1291–1292.
- McKeon A, Martinez-Hernandez E, Lancaster E, et al. Glycine receptor autoimmune spectrum with stiff-man syndrome phenotype. *JAMA Neurol* 2013;70:44–50.
- Dalmaj J, Geis C, Graus F. Autoantibodies to synaptic receptors and neuronal cell surface proteins in autoimmune diseases of the central nervous system. *Physiol Rev* 2017;97:839–887.
- Bode A, Lynch JW. The impact of human hyperekplexia mutations on glycine receptor structure and function. *Mol Brain* 2014;7:2.
- Baizabal-Carvallo JF, Jankovic J. Stiff-person syndrome: insights into a complex autoimmune disorder. *J Neurol Neurosurg Psychiatry* 2015;86:840–848.
- Geis C, Beck M, Jablonka S, et al. Stiff person syndrome associated anti-amphiphysin antibodies reduce GABA associated [Ca²⁺]_i rise in embryonic motoneurons. *Neurobiol Dis* 2009;36:191–199.
- Meinck HM, Thompson PD. Stiff man syndrome and related conditions. *Mov Disord* 2002;17:853–866.
- Sommer C, Weishaupt A, Brinkhoff J, et al. Paraneoplastic stiff-person syndrome: passive transfer to rats by means of IgG antibodies to amphiphysin. *Lancet* 2005;365:1406–1411.
- Alexopoulos H, Akrivou S, Dalakas MC. Glycine receptor antibodies in stiff-person syndrome and other GAD-positive CNS disorders. *Neurology* 2013;81:1962–1964.

14. Crisp SJ, Dixon CL, Jacobson L, et al. Glycine receptor autoantibodies disrupt inhibitory neurotransmission. *Brain* 2019;142:3398–3410.
15. Malosio ML, Marqueze-Pouey B, Kuhse J, Betz H. Widespread expression of glycine receptor subunit mRNAs in the adult and developing rat brain. *EMBO J* 1991;10:2401–2409.
16. Lynch JW. Molecular structure and function of the glycine receptor chloride channel. *Physiol Rev* 2004;84:1051–1095.
17. Lynch JW. Native glycine receptor subtypes and their physiological roles. *Neuropharmacology* 2009;56:303–309.
18. Kneussel M, Betz H. Clustering of inhibitory neurotransmitter receptors at developing postsynaptic sites: the membrane activation model. *Trends Neurosci* 2000;23:429–435.
19. Du J, Lu W, Wu S, et al. Glycine receptor mechanism elucidated by electron cryo-microscopy. *Nature* 2015;526:224–229.
20. Huang X, Chen H, Michelsen K, et al. Crystal structure of human glycine receptor- α 3 bound to antagonist strychnine. *Nature* 2015;526:277–280.
21. Huang X, Shaffer PL, Ayube S, et al. Crystal structures of human glycine receptor α 3 bound to a novel class of analgesic potentiators. *Nat Struct Mol Biol* 2017;24:108–113.
22. Doppler K, Schleyer B, Geis C, et al. Lockjaw in stiff-person syndrome with autoantibodies against glycine receptors. *Neurol Neuroimmunol Neuroinflamm* 2016;3:e186.
23. Buchwald B, Weishaupt A, Toyka KV, Dudel J. Pre- and postsynaptic blockade of neuromuscular transmission by Miller-Fisher syndrome IgG at mouse motor nerve terminals. *Eur J Neurosci* 1998;10:281–290.
24. Fuhrmann JC, Kins S, Rostaing P, et al. Gephyrin interacts with dynein light chains 1 and 2, components of motor protein complexes. *J Neurosci* 2002;22:5393–5402.
25. Farrell B, Godwin J, Richards S, Warlow C. The United Kingdom transient ischaemic attack (UK-TIA) aspirin trial: final results. *J Neurol Neurosurg Psychiatry*. 1991;54:1044–1054.
26. Chen C, Okayama H. High-efficiency transformation of mammalian cells by plasmid DNA. *Mol Cell Biol* 1987;7:2745–2752.
27. Breiting U, Breiting HG, Bauer F, et al. Conserved high affinity ligand binding and membrane association in the native and refolded extracellular domain of the human glycine receptor α 1-subunit. *J Biol Chem* 2004;279:1627–1636.
28. Sontheimer H, Becker CM, Pritchett DB, et al. Functional chloride channels by mammalian cell expression of rat glycine receptor subunit. *Neuron* 1989;2:1491–1497.
29. Schaefer N, Berger A, van Brederode J, et al. Disruption of a structurally important extracellular element in the glycine receptor leads to decreased synaptic integration and signaling resulting in severe startle disease. *J Neurosci* 2017;37:7948–7961.
30. Schindelin J, Rueden CT, Hiner MC, Eliceiri KW. The ImageJ ecosystem: an open platform for biomedical image analysis. *Mol Reprod Dev* 2015;82:518–529.
31. Ogino K, Yamada K, Nishioka T, et al. Phosphorylation of gephyrin in zebrafish Mauthner cells governs glycine receptor clustering and behavioral desensitization to sound. *J Neurosci* 2019;39:8988–8997.
32. Deckert J, Weber H, Villmann C, et al. GLRB allelic variation associated with agoraphobic cognitions, increased startle response and fear network activation: a potential neurogenetic pathway to panic disorder. *Mol Psychiatry* 2017;22:1431–1439.
33. Schaefer N, Kluck CJ, Price KL, et al. Disturbed neuronal ER-Golgi sorting of unassembled glycine receptors suggests altered subcellular processing is a cause of human hyperekplexia. *J Neurosci* 2015;35:422–437.
34. Spurny R, Debaveye S, Farinha A, et al. Molecular blueprint of allosteric binding sites in a homologue of the agonist-binding domain of the α 7 nicotinic acetylcholine receptor. *Proc Natl Acad Sci U S A* 2015;112:E2543–E2552.
35. Budick SA, O'Malley DM. Locomotor repertoire of the larval zebrafish: swimming, turning and prey capture. *J Exp Biol* 2000;203(pt 17):2565–2579.
36. Hirata H, Ogino K, Yamada K, et al. Defective escape behavior in DEAH-box RNA helicase mutants improved by restoring glycine receptor expression. *J Neurosci* 2013;33:14638–14644.
37. Saint-Amant L, Drapeau P. Time course of the development of motor behaviors in the zebrafish embryo. *J Neurobiol* 1998;37:622–632.
38. Balint B, Vincent A, Meinck HM, et al. Movement disorders with neuronal antibodies: syndromic approach, genetic parallels and pathophysiology. *Brain* 2018;141:13–36.
39. Crisp SJ, Balint B, Vincent A. Redefining progressive encephalomyelitis with rigidity and myoclonus after the discovery of antibodies to glycine receptors. *Curr Opin Neurol* 2017;30:310–316.
40. Borellini L, Lanfranconi S, Bonato S, et al. Progressive encephalomyelitis with rigidity and myoclonus associated with anti-GlyR antibodies and Hodgkin's lymphoma: a case report. *Front Neurol* 2017;8:401.
41. Brenner T, Sills GJ, Hart Y, et al. Prevalence of neurologic autoantibodies in cohorts of patients with new and established epilepsy. *Epilepsia* 2013;54:1028–1035.
42. De Blauwe SN, Santens P, Vanopdenbosch LJ. Anti-glycine receptor antibody mediated progressive encephalomyelitis with rigidity and myoclonus associated with breast cancer. *Case Rep Neurol Med* 2013;2013:589154.
43. Zuliani L, Ferlazzo E, Andriago C, et al. Glycine receptor antibodies in 2 cases of new, adult-onset epilepsy. *Neurol Neuroimmunol Neuroinflamm* 2014;1:e16.
44. Castillo-Gomez E, Oliveira B, Tapken D, et al. All naturally occurring autoantibodies against the NMDA receptor subunit NR1 have pathogenic potential irrespective of epitope and immunoglobulin class. *Mol Psychiatry* 2017;22:1776–1784.
45. Atak S, Langlhofer G, Schaefer N, et al. Disturbances of ligand potency and enhanced degradation of the human glycine receptor at affected positions G160 and T162 originally identified in patients suffering from hyperekplexia. *Front Molec Neurosci* 2015;8:79.
46. Villmann C, Oertel J, Melzer N, Becker CM. Recessive hyperekplexia mutations of the glycine receptor α 1 subunit affect cell surface integration and stability. *J Neurochem* 2009;111:837–847.
47. Bode A, Wood SE, Mullins JG, et al. New hyperekplexia mutations provide insight into glycine receptor assembly, trafficking, and activation mechanisms. *J Biol Chem* 2013;288:33745–33759.
48. Chung SK, Vanbellinghen JF, Mullins JG, et al. Pathophysiological mechanisms of dominant and recessive GLRA1 mutations in hyperekplexia. *J Neurosci* 2010;30:9612–9620.
49. Saul B, Kuner T, Sobetzko D, et al. Novel GLRA1 missense mutation (P250T) in dominant hyperekplexia defines an intracellular determinant of glycine receptor channel gating. *J Neurosci* 1999;19:869–877.
50. Zhang Y, Bode A, Nguyen B, et al. Investigating the mechanism by which gain-of-function mutations to the α 1 glycine receptor cause hyperekplexia. *J Biol Chem* 2016;291:15332–15341.
51. Ganser LR, Yan Q, James VM, et al. Distinct phenotypes in zebrafish models of human startle disease. *Neurobiol Dis* 2013;60:139–151.
52. Hirata H, Saint-Amant L, Downes GB, et al. Zebrafish bandoneon mutants display behavioral defects due to a mutation in the glycine receptor β -subunit. *Proc Natl Acad Sci U S A* 2005;102:8345–8350.
53. Leacock S, Syed P, James VM, et al. Structure/function studies of the α 4 subunit reveal evolutionary loss of a GlyR subtype involved in startle and escape responses. *Front Mol Neurosci* 2018;11:23.
54. Stengel H, Vural A, Brunder AM, et al. Anti-pan-neurofascin IgG3 as a marker of fulminant autoimmune neuropathy. *Neurol Neuroimmunol Neuroinflamm* 2019;6:e603.